

## Experimental investigation of a Brownian ratchet effect in ferrofluids

Thomas John and Ralf Stannarius

*Institut für Experimentelle Physik, Fakultät für Naturwissenschaften, Universität Magdeburg, Universitätsplatz 2, D-39106 Magdeburg, Germany*

(Received 3 February 2009; revised manuscript received 24 August 2009; published 25 November 2009)

We test experimentally a Brownian ratchet system suggested by Engel *et al.* [Phys. Rev. Lett. **91**, 060602 (2003)]. This ratchet system is based on a magnetic fluid that contains nanometer sized magnetic particles in a thermal bath of carrier fluid. An external static magnetic field and, perpendicular to it, an oscillatory magnetic field act on the ferrofluid particles; the total magnetic field contains no rotating component. The directed effective rotation of the particles due to the ratchet effect induces a macroscopic torque density of the fluid. The torque on a spherical ferrofluid sample is measured in dependence on the field parameters. A quantitative comparison with predictions from a microscopic and a phenomenological model are given. Both models describe certain aspects of the measurements correctly, but qualitative discrepancies between both models and experiment are found, particularly in the high-frequency range.

DOI: [10.1103/PhysRevE.80.050104](https://doi.org/10.1103/PhysRevE.80.050104)

PACS number(s): 05.40.Jc, 47.65.Cb

The extraction of energy or a directed force from random thermal motion of particles is an old controversially discussed problem in statistical physics. It started with Maxwell's intelligent Daemon [1] and was later abstracted by Smoluchowski using a mechanical ratchet system. References [2–4], e.g., give overviews of Brownian motors. The Brownian-driven directed motion of microscopic objects is consistent with the second law of thermodynamics if the system is driven far from equilibrium [5]. The basic components of such ratchets are a thermal bath and the Brownian motion of the objects in an asymmetric time-periodic potential. We study ferrofluids in an external magnetic field, suggested by Engel *et al.* [6], as a model system for a Brownian ratchet. Ferrofluids as stable suspensions of nanometer sized magnetic monodomain particles in a carrier fluid (see, e.g., [7]) are well suited for such investigations because the particles are strongly affected by thermal fluctuations and their individual particle orientations can be influenced by an external magnetic field. Simultaneous influences on the orientations of all particles lead to changes in macroscopic material properties, a static field, e.g., leads to the classical Langevin magnetization  $\vec{M}(\vec{H})$  [8], alternating fields can reduce the viscosity of the fluid down to an effective “negative viscosity” [9–11]. In our ratchet system we use a superposition of a static and an alternating magnetic field to break the symmetry of clockwise and counterclockwise reorientations of the particles in the plane of the magnetic field. This leads to an effective directed rotation measured as an induced torque density in the sample because of the viscous coupling of the particles to the carrier fluid. We mention in passing that our superimposed field is not rotating, in contrast to that in the experiments by Chaves *et al.* [12].

In presence of a static field  $H_x$  in  $x$  direction, the particles have a preferential orientation but no preferred direction of orientational fluctuations from a microscopic point of view. However, if the static field is superimposed with a suitable time-periodic field in  $y$  direction, a ratchet potential is formed, and one measures a time-averaged net torque in  $z$  direction on the ferrofluid sample, resulting from the preference of one rotation sense. A simple suitable waveform is the

superposition of two harmonic functions [6], exemplarily

$$H_y(t) = H_{y,1} \cos(2\pi ft) + H_{y,2} \sin(4\pi ft + \delta), \quad (1)$$

where  $H_{y,1}$  and  $H_{y,2}$  are the amplitudes of the first and second harmonics of the magnetic field with period  $1/f$ . The time integral of  $H_y(t)$  over one period is zero. The phase difference  $\delta$  represents a continuous measure for the asymmetry in time. The macroscopic behavior of a ferrofluid under the influence of the above-described fields was studied by Engel *et al.* within a microscopic model [6,13]. In a comment to [6], Shliomis [14] proposed an alternative phenomenological (Debye) model. The predictions of these two models are comparable in many points, careful quantitative experiments are necessary to test their validity. Both models yield a non-zero mean torque density in the sample averaged over the excitation period  $1/f$ . However, irrespective of some similarities in the predictions, there is a big conceptual difference between both descriptions. While the first one [6] depends upon the assumption of stochastic forces and a Brownian motion in the system, the second one [14] is more general and it can be derived from a nonlinear magnetization curve alone.

We use a sensitive torsional pendulum [6,15,16] to measure the torque on the sample. The experimental data are compared with quantitative predictions of the models. The torsion pendulum setup consists of a spherical glass container of 20 mm diameter filled with the commercial ferrofluid (APG935, [17,18]). The sphere is glued to a glass fiber (diameter of 5  $\mu\text{m}$  and length of 80 cm) which is suspended from an upper support. Rotation angles  $\varphi$  of the sphere under the influence of magnetic torques are measured contactless with a video camera in a resolution of  $0.2^\circ$ . At excitation frequencies  $f \gg 1$  Hz, the pendulum with an eigenfrequency of about 40 mHz quickly adopts a quasiconstant rotation angle where the torque on the ferrofluid is counterbalanced by the fiber distortion. The slow flow of the viscous ferrofluid inside to the container can be neglected. We find a linear relation  $n = c\varphi$  between torque density per volume,  $n$ , and twist angle  $\varphi$  with a calibration constant  $c = 0.09 \mu\text{Nm}/(\ell \text{ deg})$ . The sample is in the center between

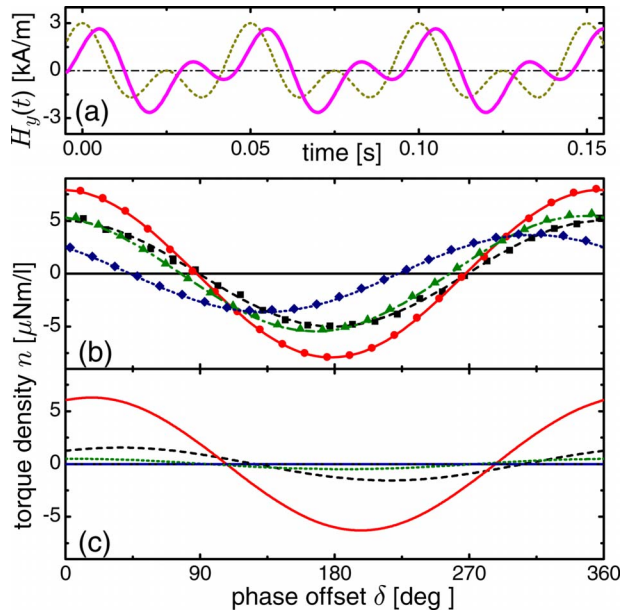


FIG. 1. (Color online) (a) Excitation field  $H_y(t)$  at phase shift  $\delta=0^\circ$  (solid line) and  $\delta=90^\circ$  (dotted line) at  $f=20$  Hz and  $H_{y,1}=H_{y,2}=1.5$  kA/m. (b) Measured torque densities at frequencies  $f=5$  Hz (dashed line), 20 Hz (solid line), 100 Hz (dash-dotted line), and 500 Hz (dotted line). The first sign reversal of  $n(\delta)$  defines the intersection point  $\delta_i$ . Lines are fitted sine functions to extract amplitudes and phases. (c) Calculated torque densities  $n(\delta)$  from the microscopic model at same frequencies and depicted in same line styles as (b). The phenomenological models predict the same sinusoidal dependencies but different amplitudes and phases, see Fig. 3.

two orthogonal pairs of Helmholtz coils (21 cm diameter for the static field  $H_x$  and 9 cm diameter for the oscillatory field  $H_y$ ). A maximum static field of 9 kA/m can be generated, the frequency range for the oscillatory field  $H_y(t)$  is 5–600 Hz, the waveform is synthesized in a function generator and amplified.

Figure 1(a) depicts typical curves for the time-dependent  $H_y$  excitation field. In Fig. 1(b), we show exemplary experimental results for the measured and in Fig. 1(c) for calculated torque densities. An important parameter of the excitation is the temporal characteristics of the oscillatory field  $H_y$ . One can tune it by variation in  $\delta$  in Eq. (1). Both models [6,14] predict  $n(\delta) \propto n_{\max} \sin(\delta - \delta_i)$  with an amplitude  $n_{\max}$  and the intersection point  $\delta_i$ . The data in Fig. 1 are in excellent agreement with the predicted sine dependence of  $n(\delta)$  for all parameter combinations. Thus we can reduce our data in the following by extracting only  $n_{\max}$  and  $\delta_i$  to characterize the torques. The experimental results confirm the intrinsic symmetry  $n(\delta_i + \delta) = -n(\delta_i - \delta)$ , as well as all other symmetries considered in the Appendix of Ref. [13]. With the extracted  $n_{\max}$  and  $\delta_i$  we characterize the frequency dependence and the other field parameter dependencies of the torque densities.

For comparison with theory, we briefly review the two descriptions in literature: in the phenomenological model [14], single particles do not play a role. The Brownian motion is reflected in the viscosity  $\eta=1.5$  Pas

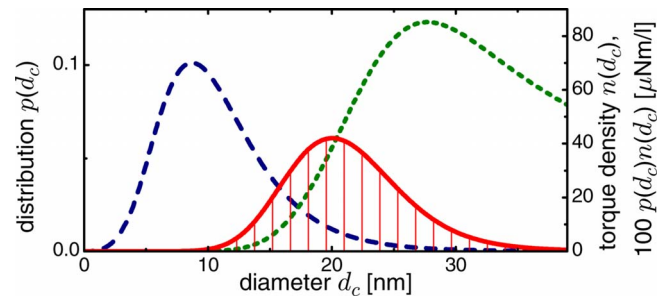


FIG. 2. (Color online) Calculated torque densities in the microscopic model from the numerical solution  $n(d_c)$  (dotted line) for monodisperse ferrofluid suspensions with given particle diameter and same saturation magnetization as APG935, parameters see text. The integral over the weighted torque distribution  $p(d_c)n(d_c)$  (solid line) with the assumed particle size distribution  $p(d_c)$  (dashed line) gives the torque density of the polydisperse ferrofluid.

of the fluid APG935, and in the Debye relaxation  $\dot{\vec{M}} = -(\vec{M} - \vec{M}^{\text{eq}})/\tau_B$ . There is a nonlinear magnetic field dependence of the equilibrium magnetization  $\vec{M}^{\text{eq}} = M_S \mathcal{L}(\alpha) \vec{\alpha} / \alpha$  with  $\vec{\alpha} = (3\chi/M_S)\vec{H}$  and the saturation magnetization  $M_S = 18$  kA/m of APG935. To achieve predictions at higher fields we calculate the torque density numerically without the series expansion of  $\vec{M}^{\text{eq}}$  in  $\vec{H}$ . At fields below 5 kA/m the analytical formula in [14] gives an excellent approximation to the numerical exact solution. In this description, only the susceptibility  $\chi$  of the ferrofluid and the Brownian relaxation time  $\tau_B$  remain as fit parameters. We use  $\chi=0.9$  and  $\tau_B=4$  ms in our calculations.

In the microscopic model, the stochastic rotation of a single particle in a viscous carrier fluid is considered. The detailed treatment in [13] calculates the contributions to the torque density by a single particle based on the biased rotation about the  $z$  axis. The magnetic moment of the particle is assumed as  $m = \mu_0 M_B \pi d_c^3 / 6$ , with the magnetic core diameter  $d_c$  and the saturation magnetization of  $M_B = 451$  kA/m of the ferromagnetic material magnetite. The Brownian relaxation time is defined by  $\tau_B = \pi \eta d_h^3 / (2k_B T)$ , with the hydrodynamic diameter  $d_h$ . The magnetic cores are coated to prevent an agglomeration, therefore we use  $d_h = d_c + 5$  nm in calculations. For the quantitative comparison of the model with experiments we could not use the asymptotic small field approximations in [13] instead the Fokker-Planck-equation has been solved numerically [27]. As mentioned in [6], the polydispersity of the ferrofluid cannot be neglected in qualitative comparisons. Thus we have expanded the numerical analysis to a noninteracting polydisperse suspension with given particle diameter distribution and a volume fraction  $M_S/M_B$ . We use a log-normal distribution with a mean of  $d_c = 10$  nm for APG935 and a standard deviation of  $\sigma = 1.5$ , see independent measurements in Ref. [18]. The calculated torque density  $n(d_c)$  for a polydisperse ferrofluid with the saturation magnetization of APG935 is shown in Fig. 2, together with the distribution  $p(d_c)$  (dashed line). Field parameters are  $H_x = H_{y,1} = H_{y,2} = \vec{H} = 1.5$  kA/m,  $f = 30$  Hz, and  $\delta = 0$ . The predicted torque density of a polydisperse ferrofluid is the integral of  $p(d_c)n(d_c)$  (solid line)

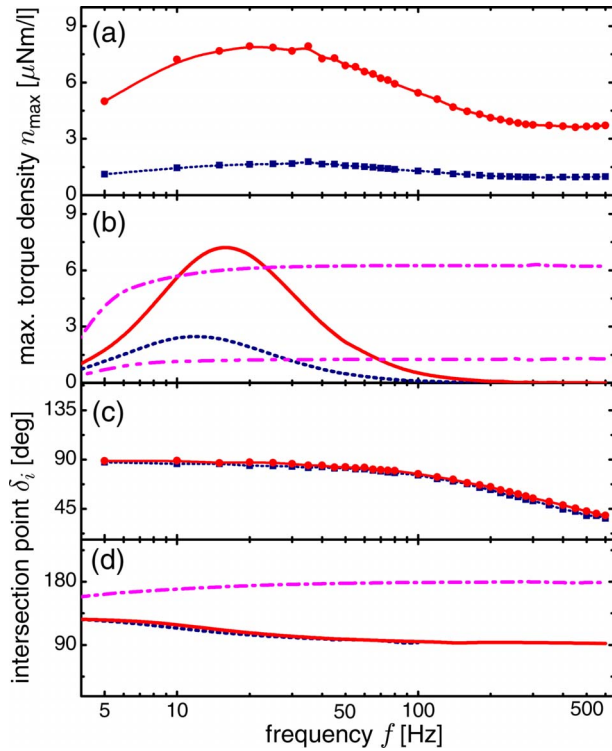


FIG. 3. (Color online) [(a) and (c)] Measured and [(b) and (d)] calculated maximal amplitudes of the [(a) and (b)] torque densities  $n_{\max}$  and [(c) and (d)] intersection points  $\delta_i$  as function of the exiting frequency  $f$  in  $H_y(t)$  at magnetic field amplitudes at  $H_x = H_{y,1} = H_{y,2} = 1.5$  kA/m (solid line, circles), 1 kA/m (dotted line, squares), microscopic model (solid line, dashed line), and phenomenological model (dash dotted line, dash dot dot line), respectively. A resonance frequency at 16 Hz in microscopic model and 30 Hz in measurements can be identified.

over  $d_c$ . The ratchet is particularly effective if the particle size is larger than 10 nm (Fig. 2, dotted line), APG935 consists mainly of particles much smaller than the optimum size. An obvious conclusion is that small changes in the assumed mean particle diameter (which is difficult to access directly in experiments) in the model result in dramatic changes in the predicted total torque density. For a quantitative comparison of model and experiment, we have assumed a mean diameter  $d_c$  with a standard deviation  $\sigma$  that gives a maximum torque density magnitude comparable to the experimental results. It appears to be realistic, see below.

A maximum torque is expected near an (effective) frequency  $2\pi/\tau_B$  [6]. Data for two field strengths  $\tilde{H}=1$  and 1.5 kA/m are shown in Fig. 3. The qualitative prediction  $n \propto \tilde{H}^4$  of both models is confirmed, but the measured frequency dependence agrees qualitatively better with the phenomenological model of Shliomis [14]. In the microscopic model, the torque should drop to zero rapidly with increasing frequency. The intersection points have a characteristic frequency dependence  $\delta_i(f)$  [Figs. 3(c) and 3(d)]. Such a frequency dependence is predicted by the models. However, frequency dependencies of the  $\delta_i$  differ considerably. The values predicted in the models are above  $90^\circ$ , whereas the experimental values are all below  $90^\circ$ . The phase shift  $90^\circ$

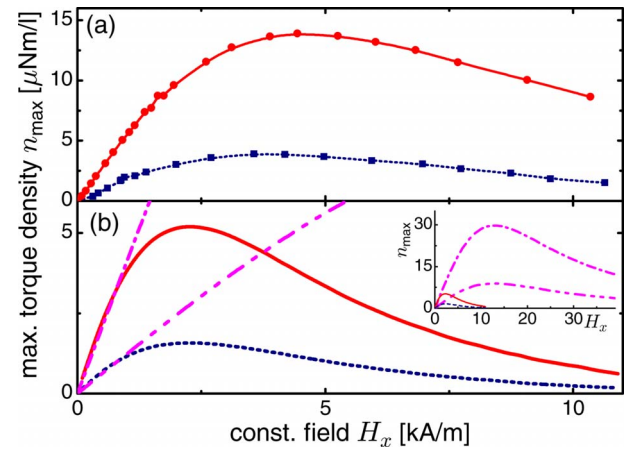


FIG. 4. (Color online) (a) Measured maximum torque densities as function of static magnetic field amplitudes  $H_x$  and  $H_{y,1} = H_{y,2} = 1.5$  kA/m (solid lines, circles) and 1 kA/m (dotted lines, squares) at  $f = 30$  Hz. Lines guide the eyes. (b) Respectively, calculated torque densities with the microscopic model [13] (solid line, dotted line), phenomenological model [14] (dash dotted, dash dot dot line). The inset in (b) depicts the same zoomed out.

marks a time-reversal symmetric waveform, which represents the frequency-independent intersection point in the simplified two-dimensional model [13]. The ferrofluid ratchet has the remarkable property that for certain excitation potentials (fixed  $\delta$ ), one can reverse the sign of induced torque by changing the frequency of the excitation [e.g., at  $\delta \approx 70^\circ$  in Fig. 1(b)].

Another interesting parameter is the field strength at fixed excitation shape. In the microscopic view, the stochastic motion is covered by the deterministic motion at strong fields and the induced torque should decrease. In terms of energies, the magnetic potential wall exceeds the thermal energy  $k_B T$ , and the system behaves as “frozen.” By experimental limitations, we can only increase the static field to sufficiently high amplitudes. The dependence of  $n(H_x)$  at fixed  $H_{y,1}$ ,  $H_{y,2}$  is shown in Fig. 4. The linear increment of  $n(H_x)$  at low  $H_x$  predicted by both models is confirmed in the experiment. The decrease at higher field strength, as observed in the experiment, is in agreement with the microscopic and the phenomenological models [13,14], at least qualitatively.

The influence of the Brownian relaxation time has been investigated by studying two other magnetite ferrofluids, APGS21 and APGo77n [17], with lower viscosities than APG935. In both models [6,14], the Brownian relaxation time is proportional to the viscosity and a shift of the global torque maximum with frequency is expected. This can be seen in Fig. 5. For APGS21, the saturation at high frequencies is observed as well. The particle size distribution is unknown for all investigated ferrofluids, therefore one cannot compare these measurements to the models on a quantitative level.

In summary, we have presented the first quantitative experimental study of a Brownian ratchet in ferrofluids and compared the experimental data with models. Both models describe macroscopic torques on the ferrofluid quantitatively correctly in certain parameter ranges, but globally there are

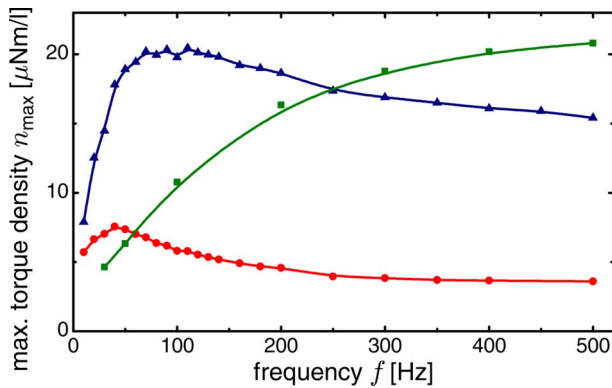


FIG. 5. (Color online) Amplitudes of measured maximum torque densities  $n_{\max}(f)$  at a field strength of  $\tilde{H}=1.5$  kA/m for three ferrofluids, APG935 with viscosity  $\eta=1.5$  Pas (circles), APGS21 with  $\eta=0.5$  Pas (triangles), and APGo77n with  $\eta=0.1$  Pas (squares). Lines guide the eyes.

even qualitative discrepancies. The first one concerns the high-frequency behavior which is not predicted correctly, neither from the microscopic nor the phenomenological model, another one is related to the absolute values and frequency characteristics of the inversion points  $\delta_i$  where the torque changes sign. We conclude that neither the micro-

scopic [6] nor the phenomenological [14] models in the current state provide a satisfactory quantitative description of the effect. On the other hand, the measured apparent saturation of the torque at high frequencies cannot be explained within the microscopic model. We have checked also an expansion of the model which allows for particle-particle interactions [19]. The predicted high-frequency behavior remains nonsatisfactory. A deeper theoretical understanding of the basic mechanisms is desirable. Other magnetization functions could be helpfully, e.g., the *effective field theory* by Shliomis [9,20], the *ferrofluid dynamics approach* from Müller *et al.* [21] or Felderhof's approach [22]. Also the known chain formation process [23,24] can be imported for a better quantitative understanding. The correct dynamics of ferrofluids is an open issue [25] and the ratchet experiment should provide the basis for more realistic modeling. An interesting aspect of this ratchet system is the sign inversion of the ratchet effect for certain fixed excitation wave forms [certain fixed  $\delta$  in Eq. (1), which is analogous to observations in translatory systems [26]]. Our measurements, at the present stage, cannot unambiguously distinguish between the two models in literature [6,14] but underline the shortcomings of both concepts in the description of the experiment.

The authors acknowledge A. Engel, V. Becker, and A. Leschhorn for fruitful and stimulating discussions.

- [1] J. C. Maxwell, *Theory of Heat* (Longmans, Green, London, 1871).
- [2] M. V. Smoluchowski, *Phys. Z.* **13**, 1069 (1912).
- [3] P. Reimann, *Phys. Rep.* **361**, 57 (2002).
- [4] R. D. Astumian, *Science* **276**, 917 (1997).
- [5] R. P. Feynman, R. B. Leighton, and M. Sands, *Lectures on Physics* (Addison-Wesley, Reading, MA, 1963), Vol. 1.
- [6] A. Engel, H. W. Müller, P. Reimann, and A. Jung, *Phys. Rev. Lett.* **91**, 060602 (2003).
- [7] *Colloidal Magnetic Fluids*, Lecture Notes in Physics Vol. 763, edited by S. Odenbach (Springer, New York, 2009).
- [8] R. E. Rosensweig, *Ferrohydrodynamics* (Cambridge University Press, Cambridge, England, 1985).
- [9] J.-C. Bacri, R. Perzynski, M. I. Shliomis, and G. I. Burde, *Phys. Rev. Lett.* **75**, 2128 (1995).
- [10] A. Zeuner, R. Richter, and I. Rehberg, *Phys. Rev. E* **58**, 6287 (1998).
- [11] R. Krauß, B. Reimann, R. Richter, I. Rehberg, and M. Liu, *Appl. Phys. Lett.* **86**, 024102 (2005).
- [12] A. Chaves, C. Rinaldi, S. Elborai, X. He, and M. Zahn, *Phys. Rev. Lett.* **96**, 194501 (2006).
- [13] A. Engel and P. Reimann, *Phys. Rev. E* **70**, 051107 (2004).
- [14] M. I. Shliomis, *Phys. Rev. Lett.* **92**, 188901 (2004).
- [15] M. I. Shliomis and M. A. Zaks, *Phys. Rev. E* **73**, 066208 (2006).
- [16] M. I. Shliomis and M. A. Zaks, *Phys. Rev. Lett.* **93**, 047202 (2004).
- [17] We used commercial audio-ferrofluid APG935, APGS21 and APGo77n, for material parameters see also www.ferrotec.com
- [18] J. Embs, H. W. Müller, C. E. Krill, F. Meyer, H. Natter, B. Müller, S. Wiegand, M. Lücke, K. Knorr, and R. Hempelmann, *Z. Phys. Chem.* **220**, 153 (2006).
- [19] V. Becker and A. Engel, *Phys. Rev. E* **75**, 031118 (2007).
- [20] M. I. Shliomis, *Sov. Phys. JETP* **34**, 1291 (1972).
- [21] H. W. Müller and M. Liu, *Phys. Rev. E* **64**, 061405 (2001).
- [22] B. U. Felderhof, *Phys. Rev. E* **62**, 3848 (2000).
- [23] A. Y. Zubarev and L. Y. Iskakova, *Phys. Rev. E* **61**, 5415 (2000).
- [24] S. Mahle, P. Ilg, and M. Liu, *Phys. Rev. E* **77**, 016305 (2008).
- [25] H. W. Müller and M. Liu, *Phys. Rev. E* **67**, 043202 (2003).
- [26] B. Yan, R. M. Miura, and Y. Chen, *J. Theor. Biol.* **210**, 141 (2001).
- [27] The correct fundamental Eq. (35) in [13] is
- $$\begin{aligned} \partial_t A_{l,m} = & -[H_x - iH_y(t)]/2[h_1(l-1, m-1)A_{l-1, m-1} \\ & + h_2(l+1, m-1)A_{l+1, m-1}] \\ & + [H_x + iH_y(t)]/2[h_1(l-1, -m-1)A_{l-1, m+1} \\ & + h_2(l+1, -m-1)A_{l+1, m+1}] - Dl(l+1)A_{l,m}(t); \end{aligned}$$
- V. Becker (private communication).